# Multiwavelets in the Context of Hierarchical Stereo Correspondence Matching Techniques

Pooneh Bagheri Zadeh and Cristian V. Serdean
Department of Engineering, Faculty of Technology,
De Montfort University
Leicester, UK
E-mail: pbz@dmu.ac.uk , cvs@dmu.ac.uk

***Abstract*—**This paper presents an evaluation of different types and families of multiwavelets in stereo correspondence matching. First, the paper introduces two hierarchical stereo matching techniques based on balanced and respectively unbalanced multiwavelet transforms, which employ normalized cross correlation to search for disparities. Different multiwavelet families, with different properties and filter types are evaluated, such as balanced versus unbalanced multiwavelets and symmetric-symmetric versus symmetric-antisymmetric multiwavelets. Each approximation subband carries a different spectral content of the original image and the information in the basebands of the multiwavelet transform is less sensitive to the shift variability of the multiwavelet transform. This can be exploited in order to improve the accuracy of the initial disparity map. As this initial disparity map is estimated at the lowest resolution, it needs to be progressively propagated to higher resolution levels. As a result, the search at high resolution levels is significantly reduced, thereby reducing the computational cost of the overall process and improving the reliability of the final disparity map. The evaluation of different types and families of multiwavelets shows that unbalanced multiwavelets produce a smoother disparity map with less mismatch errors compared to balanced multiwavelets. Finally, the paper introduces a third technique, which replaces normalized cross correlation with a better performing global error energy minimization algorithm operating based on a similar hierarchical technique. The results show that the multiwavelet techniques produce a smoother disparity map with less mismatch errors compared to applying a similar matching algorithm in either the spatial and/or the wavelet domains. The performance of the proposed algorithms is also compared against several state-of-the-art techniques from the Middlebury database.

***Keywords- Multiwavelets, Correspondence matching, Disparity estimation, Stereo vision.***

## I. INTRODUCTION

Stereo correspondence is an issue of great importance in the field of computer vision and 3D reconstruction. It aims to find the closest possible match between the corresponding points of two images captured simultaneously by two cameras placed at slightly different spatial locations. The cameras are usually aligned in such a way that each scan line of the rectified images corresponds to the same line in the other image, hence searching for the best correspondence match is restricted to a horizontal search. A disparity map generated from the correspondence matching process, along with the stereo camera parameters are then used to calculate the depth map and produce a 3D view of the scene. Various constraints can be taken into account in order to improve the accuracy. Even so, the accuracy of the correspondence map, which is crucial in generating a precise 3D view of the scene, is limited due to a number of problems such as occlusion, ambiguity, illumination variation and radial distortion [2].

Area-based (local) and energy-based (global) correspondence matching algorithms are the two most common types of algorithms used in the literature to generate disparity maps. In area-based methods a disparity vector for each pixel within a window search area is calculated using a matching algorithm, while in energy-based methods, the disparity vector is determined using a global cost function minimization technique. Area-based methods are fast but produce descent results, while the global methods are time consuming and generating more accurate results.

Muhlman et al. [3] presented an area-based matching technique for RGB stereo images. This algorithm uses left to right consistency and uniqueness constrains to generate the initial disparity map. The resulting disparity map is then further smoothed by applying a median filter. Another area-based scheme was proposed by Stefano et al. [4]. Stefano's algorithm is based on uniqueness and constraint, but it relies on a left to right matching phase. Yoon et al. [5] introduced a local correlation based correspondence matching technique, which uses a refined implementation of the Sum of Absolute Differences (SAD) criteria and a left to right consistency check. This algorithm uses a variable correlation window size to reduce the errors in the areas containing blurring or mismatch errors. Yoon and Kweon [6] proposed another local based algorithm, which uses different supporting weights based on the colour similarity and the geometric distances of each pixel in the search area in order to reduce the amount of ambiguity errors.

Kim et al. [7] reported a global-based technique for stereo correspondence matching. This algorithm first generates a dense disparity map using a region dividing technique based on Canny edge detection. It then further

refines the disparity map by minimizing the energy function using a Lagrangian optimization algorithm. Ogale and Aloimonos [8] proposed another global-based correspondence matching algorithm, which is independent of the contrast variation of the stereo images. This algorithm relies on multiple spatial frequency channels for local matching and a fast non-iterative left/right diffusion process for the global solution. An energy-based algorithm for stereo matching, which uses a belief propagation algorithm, was presented in [9]. This algorithm uses hierarchical belief propagation to iteratively optimize the smoothness of the disparity map. It delivers fast convergence by removing redundant computations. Choi and Jeong [10] proposed an energy-based stereo matching technique, which models the intensity differences between the two stereo images using a uniform local bias assumption. This local bias assumption is less sensitive to the intensity dissimilarity between the stereo images when using normalized crosscorrelation matching cost functions. The resulting information from the cost function is used in conjunction with a fast belief propagation algorithm to generate a smooth disparity map.

Over the past years much research has been done to improve the performance of the correspondence matching techniques. Multiresolution based stereo matching algorithms have received much attention due to the hierarchical and scale-space localization properties of the wavelets [11][13]. This allows for correspondence matching to be performed on a coarse-to-fine basis, resulting in decreased computational costs. Jiang and et al. proposed a wavelet based stereo image pair coding algorithm [14]. A wavelet transform decomposes the images into low and high frequency subbands and the disparity map is estimated using both the approximation and edge information. This is followed by a disparity compensation and subspace projection technique to improve the disparity map estimation. Caspary and Zeevi [15] presented another wavelet based stereo matching technique. This algorithm employs a differential operator in the wavelet domain to iteratively minimize a defined cost function. Sarkar and Bansal [13] presented a multiresolution based correspondence matching technique using a mutual information algorithm. They showed that the multiresolution technique produces significantly more accurate matching results compared to correlation based algorithms at much lower computational cost.

Research has shown that unlike scalar wavelets, multiwavelets can possess orthogonality (preserving length), symmetry (good performance at the boundaries via linear-phase), and a high approximation order at the same time [12], which could potentially increase the accuracy of correspondence matching techniques. Bhatti and Nahavandi [16] proposed a multiwavelet based stereo correspondence matching algorithm which makes use of the wavelet transform modulus maxima to generate a disparity map at the coarsest level. This is then followed by the coarse-to-fine strategy to refine the disparity map up to the finest level. Bagheri Zadeh and Serdean [1] proposed another multiwavelet based stereo correspondence matching technique. They used a global error energy minimization technique to find the best correspondence points between the same multiwavelet's lowest frequency subbands of the stereo pair, followed by a fuzzy algorithm to form a dense disparity map.

In spite of their highly desirable properties compared to scalar wavelets, literature surveys show that the application of multiwavelets in stereo correspondence matching has received relatively little attention so far.

This paper, investigates the application of different types and families of multiwavelets in the context of stereo correspondence matching. For this purpose, a multiwavelet is first applied to the input stereo images to decompose them into a number of subbands. Normalized cross correlation is used to generate a disparity map at the coarsest level. In the case of balanced multiwavelets, as the four low frequency subbands have similar spectral content, they can be shuffled to generate a single baseband, while in the case of unbalanced multiwavelets, the resulting basebands are used to form four disparity maps and then a Fuzzy algorithm is used to combine the four maps and generate a single disparity map. Furthermore, the paper also presents a novel hierarchical, multiwavelet based stereo correspondence matching algorithm, which employs a global error energy minimization algorithm to generate a disparity map for each of the four approximation subbands of the multiwavelet transformed input stereo pair. Again, a Fuzzy algorithm is used to combine the four disparity maps and generate an initial disparity map. As in the previous techniques, the initial estimated disparity map is then refined at higher resolution levels, taking advantage of the hierarchical, multiresolution nature of the multiwavelets to efficiently generate a more accurate final disparity map. This map is further smoothed with the aid of a median filter.

The rest of the paper is organized as it follows. Section II presents a brief review of the multiwavelet transform. An evaluation of different types and families of multiwavelets in the context of stereo correspondence matching is presented in Section III. The proposed hierarchical stereo matching technique based on global error energy minimization is introduced in Section IV. Experimental results are presented and discussed in Section V, while Section VI is dedicated to the conclusions.

## II. MULTIWAVELET TRANSFORM

Multiwavelet transforms are in many ways similar to scalar wavelet transforms. Classical wavelet theory is based on the following refinement equations:

$$\phi(t) = \sum_{k=-\infty}^{k=\infty} h_k \phi(m\,t-k)$$
$$\psi(t) = \sum_{k=-\infty}^{k=\infty} g_k \psi(m\;t-k) \qquad (1)$$

where $\phi(t)$ is a scaling function, $\psi(t)$ is a wavelet function, $h_k$ and $g_k$ are scalar filters and $m$ represents the subband number. In contrast to wavelet transforms, multiwavelets

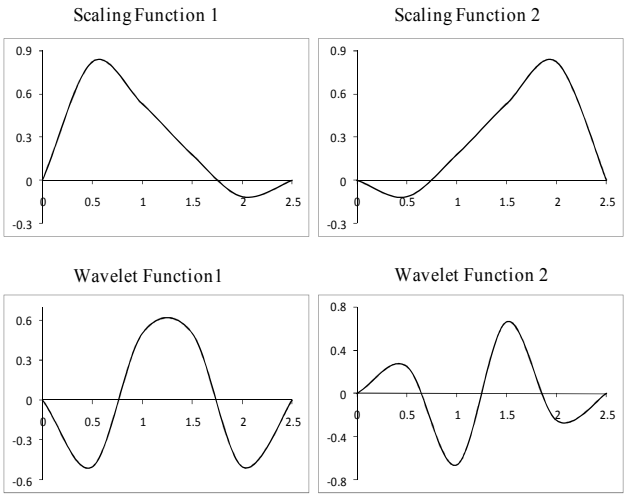


a) bat01 balanced multiwavelet

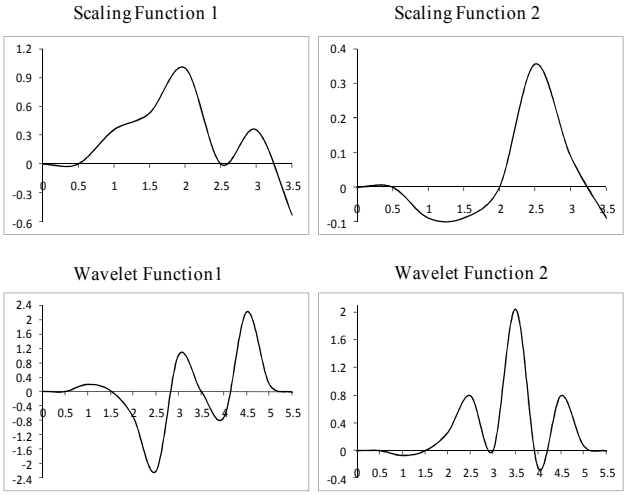


b) bih32s unbalanced multiwavelet

Figure 1. Multiwavelets basis functions, a) balanced, b) unbalanced.

have two or more scaling and respectively wavelet functions.

The set of scaling and wavelet functions of a multiwavelet in vector notation can be defined as:

$$\Phi(t) \equiv [\phi_1(t) \quad \phi_2(t) \quad \phi_3(t) \quad \dots \quad \phi_r(t)]^T$$
$$\Psi(t) \equiv [\psi_1(t) \quad \psi_2(t) \quad \psi_3(t) \quad \dots \quad \psi_r(t)]^T \qquad (2)$$

where $\Phi(t)$ and $\Psi(t)$ are the multiscaling and respectively multiwavelet functions, with $r$ scaling- and wavelet functions. In the case of scalar wavelets $r = 1$, while multiwavelets support $r \geq 2$. To date, most multiwavelets are restricted to $r = 2$. Such multiwavelets possess two scaling and two wavelet functions and can be represented as [17]:

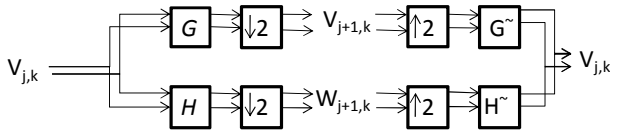


Figure 2. Analysis/synthesis stage of one level multiwavelet transform.

| | | | |
|---|---|---|---|
| $L_1L_1$ | $L_1L_2$ | $L_1H_1$ | $L_1H_2$ |
| $L_2L_1$ | $L_2L_2$ | $L_2H_1$ | $L_2H_2$ |
| $H_1L_1$ | $H_1L_2$ | $H_1H_1$ | $H_1H_2$ |
| $H_2L_1$ | $H_2L_2$ | $H_2H_1$ | $H_2H_2$ |

Figure 3. One level of 2D Multiwavelet decomposition.

$$\Phi(t) = \sqrt{2} \sum_{k=-\infty}^{k=\infty} H_k \Phi(m\,t - k)$$
$$\Psi(t) = \sqrt{2} \sum_{k=-\infty}^{k=\infty} G_k \Psi(m\,t - k) \qquad (3)$$

where $H_k$ and $G_k$ are $r \times r$ matrix filters and $m$ is the subband number. Figure 1 shows an example of balanced and unbalanced multiwavelet basis functions.

Similar to wavelet transforms, multiwavelets can be implemented using Mallat's filter bank theory [11]. Figure 2 shows one level of analysis/synthesis for a 1D multiwavelet transform, where blocks $G$ and $H$ are low- and high-pass analysis filters and $G^{\sim}$ and $H^{\sim}$ are low- and high-pass synthesis filters. Due to its separability property, a 2D multiwavelet transform can be implemented via two 1D transforms. Therefore, for one level of decomposition, a 2D multiwavelet with multiplicity $r = 2$ generates sixteen subbands, as shown in Figure 3. In Figure 3, $L_xL_y$ represent the approximation subbands while $L_xH_y$, $H_xL_y$ and $H_xH_y$ are the detail subbands, with $x = \overline{1,2}$ and $y = \overline{1,2}$.

The major advantage of multiwavelets over scalar wavelets is their ability to possess symmetry, orthogonality and higher order of approximation simultaneously, which is impossible for scalar wavelets. Furthermore, the multichannel structure of the multiwavelet transform is a closer approximation of the human visual system than what wavelets offer. In the case of unbalanced multiwavelets, the resulting approximation subbands carry different spectral content of the original image (both high- and low-frequencies), while for balanced multiwavelets, the approximation subbands contain similar spectral content of the original image [19]. This feature of unbalanced multiwavelets has the potential to increase the accuracy of

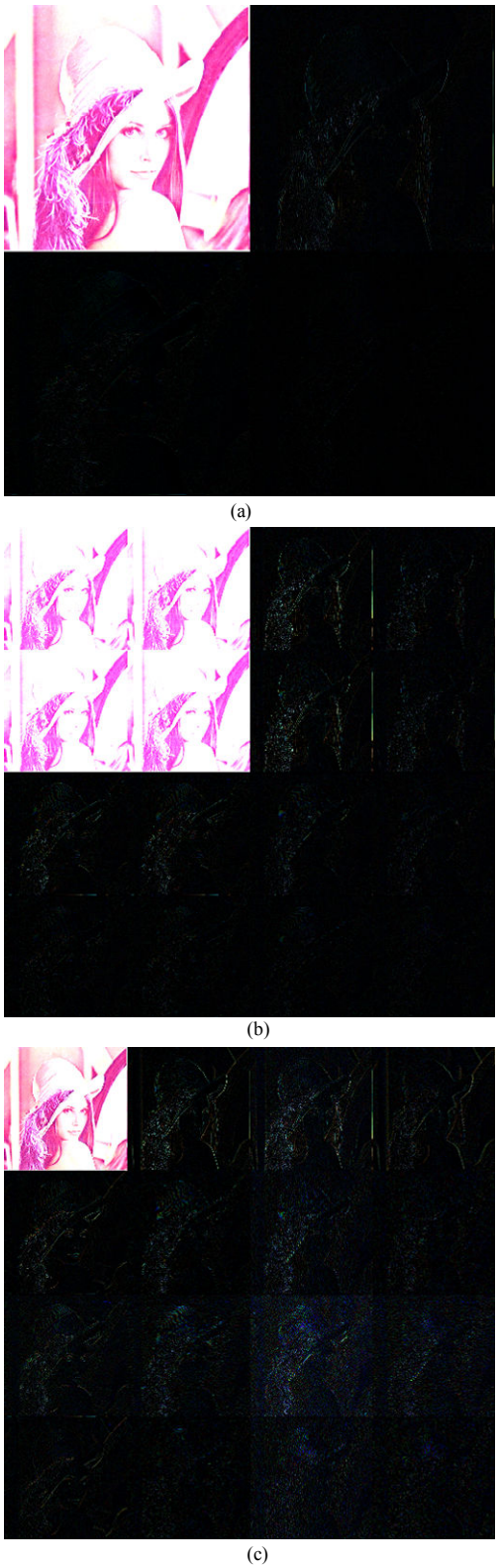

Figure 4. Single level decomposition of Lena test image (a) Antonini 9/7 wavelet transform, (b) balanced bat01 multiwavelet transform and (c) unbalanced GHM multiwavelet transform.

the calculated disparity maps and reduce the number of erroneous matches compared to that of balanced multiwavelets.

A visual comparison of the resulting subbands for a 2D wavelet, balanced and respectively unbalanced multiwavelet decomposition is shown in Figure 4. Antonini 9/7 wavelet and, balanced bat01 and unbalanced GHM multiwavelets were applied to Lena test image and results are illustrated in Figures 4(a) to 4(c), respectively. As it can be seen from Figure 4, multiwavelets generate four subbands instead of each subband that wavelets create. The resulting unbalanced multiwavelet subbands carry different spectral content of the original Lena test image, while the balanced multiwavelet subbands produce similar spectral content of the original image. More information about the generation of multiwavelets, their properties and their applications can be found in [12], [17] and [18].

## III. Evaluation of Multiwavelet Families in Stereo Correspondence Matching

The proposed stereo correspondence matching evaluation system is based on multiwavelets and normalized cross correlation. Figures 5(a) and 5(b) show the block diagrams of the proposed system for both balanced and respectively unbalanced multiwavelets. A pair of stereo images is input to the stereo matching system. The images are first rectified to suppress vertical displacement. A multiwavelet transform is then applied to each input stereo image. Different types and families of multiwavelets are evaluated. Since the information in the approximation subbands is less sensitive to the shift variability of the multiwavelets, these subbands are used in the correspondence matching process. In the case of balanced multiwavelets (Figure 5(a)), as their basebands contain similar spectral information, it is possible to use the shuffling technique proposed in [27] to rearrange the multiwavelet coefficients and generate a single low frequency subband. Figure 6 shows how four multiwavelet basebands are reshuffled to form a single baseband. Figure 6(a) shows the four multiwavelet basebands with eight pixels (two from each baseband) highlighted and given a unique numeric label. Figure 6(b) shows the same set of pixels after reshuffling, where coefficients corresponding to the same spatial locations in different basebands are placed together to generate a single baseband. Normalized cross correlation is then employed to find the best correspondence points between the two basebands of the stereo image pairs and a disparity map is generated.

Figure 5(b) shows the block diagram of the unbalanced multiwavelet based stereo matching system. While the shuffling technique works very well for balanced multiwavelets, it is not suitable for unbalanced multiwavelets due to the different spatio-frequency content of the four approximation subbands. The unbalanced multiwavelet basebands contain both high and low frequency information with $L_1L_1$ (top left baseband) containing most of the image energy. For correspondence matching purposes, the same basebands from the two views are input to the normalized cross correlation block, generating four disparity maps as a result. A Fuzzy algorithm is

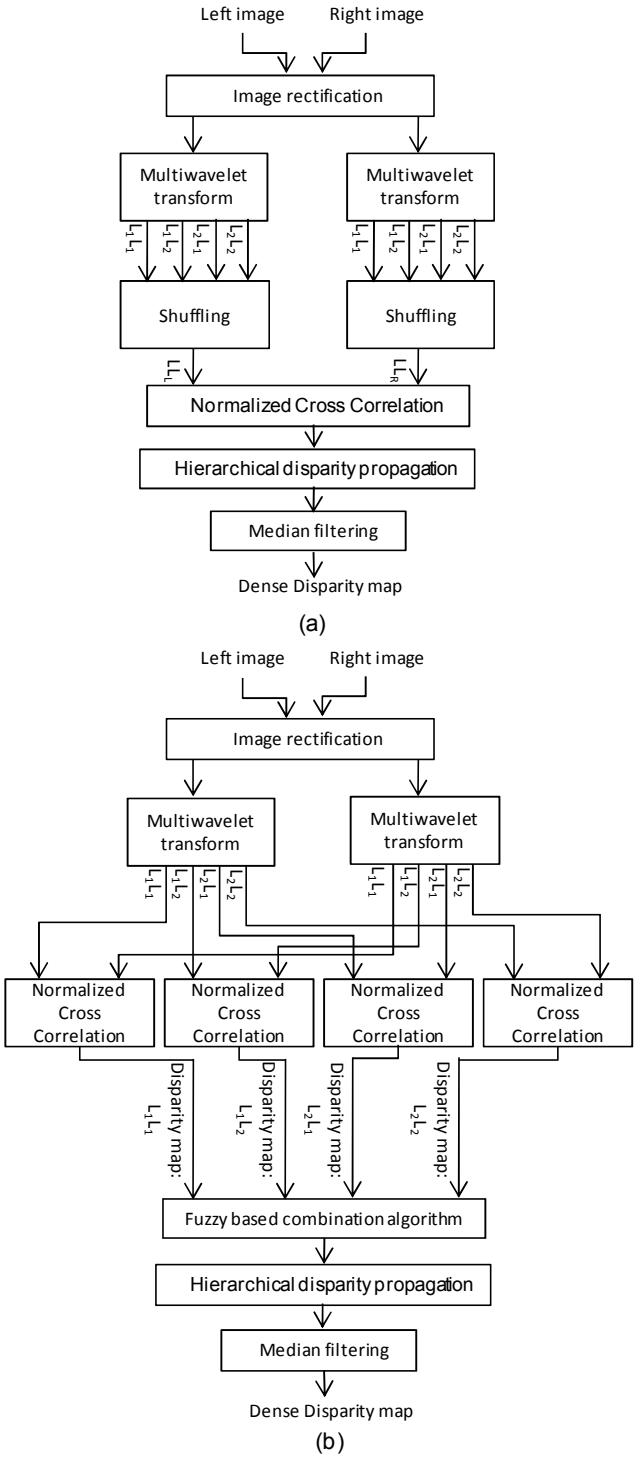


Figure 5. Block diagram of multiwavelet based stereo matching technique, for (a) balanced- and (b) unbalanced-multiwavelets.

employed to combine the four disparity maps. This algorithm gives a higher weight to the disparity values resulting from the $L_1L_1$ subbands. The disparity values in the other three disparity maps are used to refine the initial disparity map.

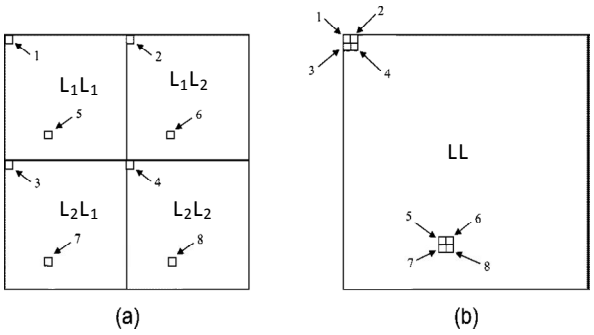


Figure 6. Shuffling method for multiwavelet baseband coefficients; selected pixels are numbered to indicate correspondence (a) before shuffling and (b) after shuffling.

These initial disparities generated at the lowest resolution for both unbalanced and balanced multiwavelets are passed on to higher resolution levels. This process is detailed in Section IV sub-section B. Finally a median filter is applied to the resulting disparity map to further smooth the resulting disparities and generate the final disparity map.

## IV. Hierarchical Multiwavelet-based Stereo Correspondence Matchning

Figure 7 shows a block diagram of the proposed hierarchical multiwavelet-based stereo matching technique which employs a global error energy minimization algorithm. A pair of rectified stereo images is input to the system. An unbalanced multiwavelet transform is then applied to the stereo images to decorrelate them into their subbands. In this paper, an unbalanced multiwavelet with a multiplicity order *r=2* is used, and as such the multiwavelet transform of each input image contains four basebands. The basebands of the unbalanced multiwavelets contain both high and low frequencies information, with $L_1L_1$ (top left baseband) containing most of the image energy. For correspondence matching purposes, the same basebands from the two views are input to a regional-based stereo matching block generating four disparity maps as a result [20]. This global error energy minimization technique is briefly described in sub-section A. The Fuzzy algorithm, which was discussed in Section III, is then employed to combine the four disparity maps. The initial disparity is estimated at the lowest resolution and the information needs to be progressively passed on to higher resolution levels. Hence, the search at high resolution levels is significantly reduced, thereby reducing the computational cost of the overall algorithm. This process is detailed in sub-section B. Finally a median filter is applied to the last processed disparity map to further smooth the final disparity map.

### *A. Global Error Energy Minimization technique*

The Global Error Energy Minimization (GEEM) technique [20] employed in this paper calculates a disparity vector for each pixel. It searches for the best match for each pixel in the correspondence search area of the other image using an error minimization criterion. For RGB images,

the error energy criteria can be defined as:

$$Er_{en}(i,j,w_x,w_y) = \frac{1}{3}\sum_{k=1}^{3}(I_1(i+w_x,j+w_y,k)-I_2(i,j,k))^2$$
$$-d_x \le w_x \le d_x \quad and \quad -d_y \le w_y \le d_y$$
$$i = 1, \ldots m \quad and \quad j = 1, \cdots n \qquad (4)$$

where $I_1$ and $I_2$ are the two input images, $Er_{en}(i,j,w_x,w_y)$ is the energy difference of the pixel $I_2(i,j)$ and pixel $I_1(i+w_x,j+w_y)$, $d_x$ is the maximum displacement around the pixel in the $x$ direction, $d_y$ is the maximum displacement around the pixel in the $y$ direction, $m$ and $n$ represent the image size and $k$ represents the three components of an RGB image.

In order for the GEEM algorithm to determine the disparity vector for each pixel in the current view, it first calculates $Er_{en}$ of each pixel with all the pixels from its search area in the corresponding image. For every disparity vector $(w_x,w_y)$ in the disparity search area, the energy of the error is calculated using Equation 4 and placed into a matrix. Each of the resulting error energy matrices is first filtered using an average filter to decrease the number of incorrect matches [21]. The disparity index of each pixel is then determined by finding the disparity index from the matrix, which contains the minimum error energy for that pixel. In order to increase the reliability of the disparity vectors around the object boundaries, which is the result of object occlusion in images, the generated disparity map undergoes a thresholding procedure as it follows:

$$\tilde{d}(i,j) = \begin{cases} d(i,j) & Er_{en}(i,j) \le \alpha \times Mean(Er_{en}) \\ 0 & Er_{en}(i,j) > \alpha \times Mean(Er_{en}) \end{cases} \qquad (5)$$

where $\tilde{d}(i,j)$ is the processed disparity map, $d(i,j)$ is the original disparity map, $\alpha$ is a tolerance reliability factor and $Er_{en}(i,j)$ is the minimum error energy of the pixel $(i,j)$ calculated and selected in the previous stage. Finally a median filter is applied to the processed disparity map $\tilde{d}(i,j)$, to further smooth the resulting final disparity map.

### B. Hierarchical disparity propagation

The information in the initial disparity map, generated at the coarsest level, needs to be refined by propagating it to the higher resolutions. Based on the wavelet theory, one point $(x,y)$ of a coarse subband in the decomposition level $i+1$ corresponds to four points $(2x,2y)$, $(2x+1,2y)$, $(2x,2y+1)$ and $(2x+1,2y+1)$ of its finer subband at the decomposition level $i$. If $(x,y)$ in the left image corresponds to $(x',y')$ in the right image at level $i+1$, $(2x,2y)$ corresponds to one of the four points $(2x',2y')$, $(2x'+1,2y')$, $(2x',2y'+1)$ and $(2x'+1,2y'+1)$ from level $i$. Hence, the disparity in level $i+1$ can be propagated to the next finer level $i$ by:

$$D_i(2x,2y) = 2D_{i+1}(x,y) + \Delta d \qquad (6)$$

where $\Delta d$ is one of $(0,0)$, $(1,0)$, $(0,1)$ and $(1,1)$, which minimizes the error of the matching metric. Disparities at the remaining points are interpolated from $D_i(2x,2y)$. A similar method has been employed in [13].

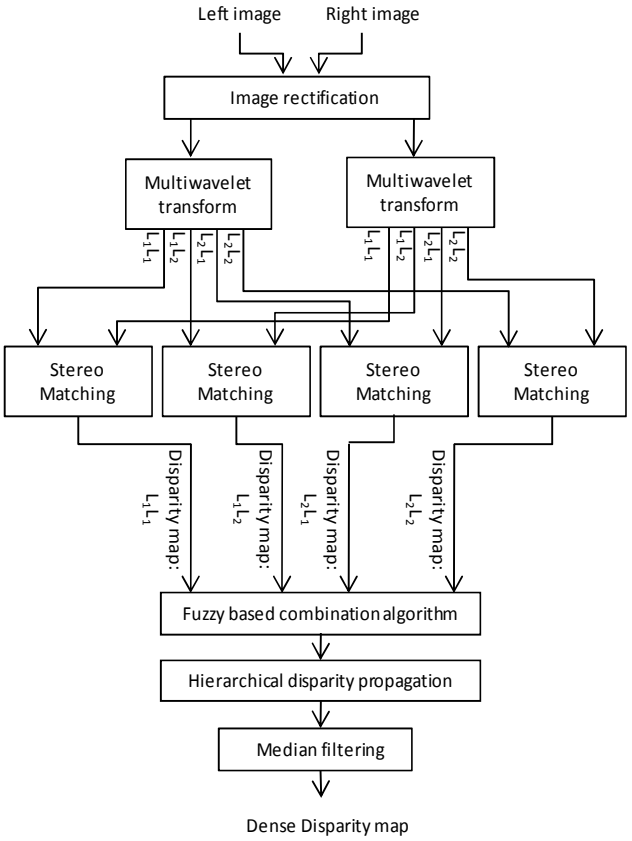


Figure 7. Block diagram of the hierarchical multiwavelet-based stereo matching technique using the global error energy minimization algorithm.

## V. Simulation Results

The performance of the proposed algorithms discussed in this paper has been assessed against the 'Cones', 'Tsukuba', 'Teddy' and 'Venus' standard stereo test images from the Middlebury stereo database [22]. Figure 8 shows the left image and the ground truth for these test images. The performance of different types and families of multiwavelets in the context of stereo correspondence matching has been evaluated using the 'Teddy' and 'Cones' stereo test images

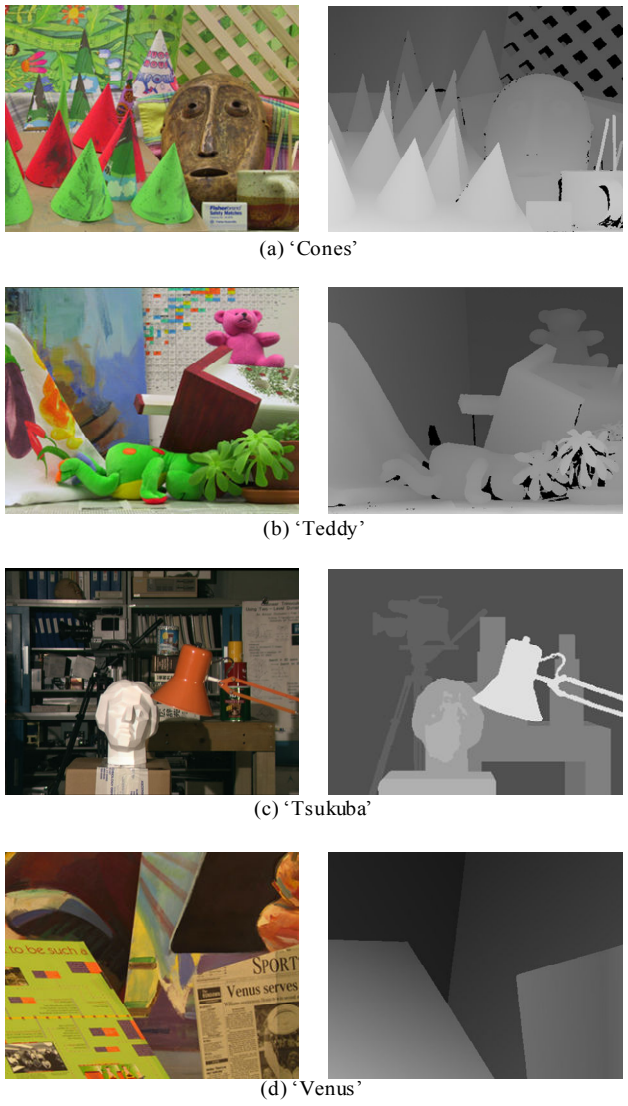


Figure 8. The left image and the ground truth of the (a) 'Cones', (b) 'Tsukuba', (c) 'Teddy' and (d) 'Venus' stereo test images.

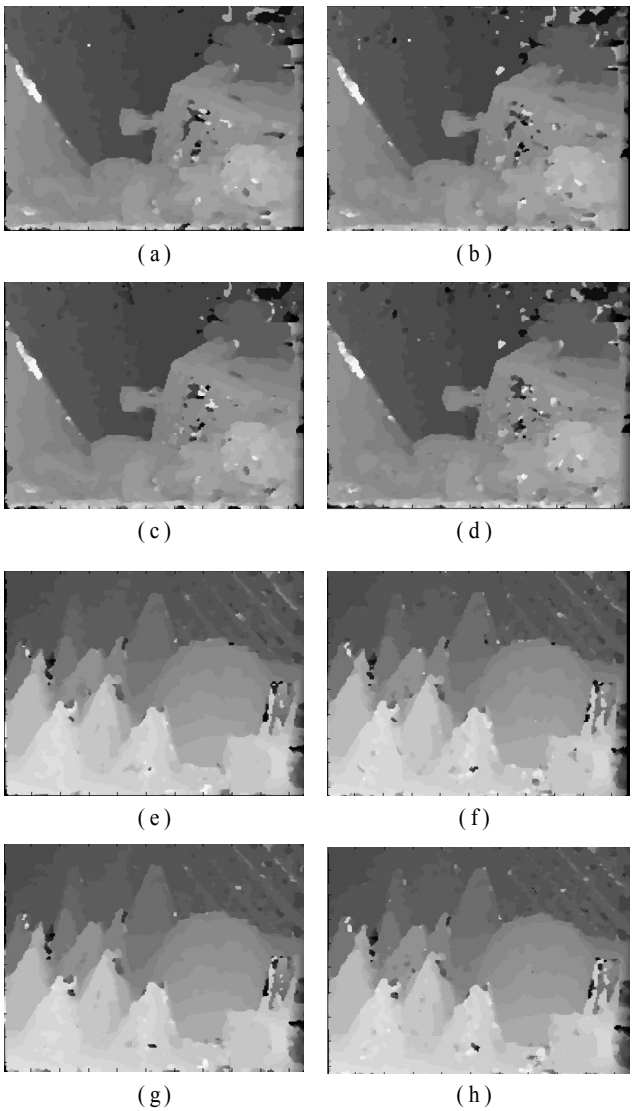


Figure 9. Disparity maps obtained by using the multiwavelet basebands of the 'Teddy' stereo test image for subbands: a) $L_1L_1$, b) $L_1L_2$, c) $L_2L_1$ and d) $L_2L_2$ and respectively 'Cones' stereo test image for subbands: e) $L_1L_1$, f) $L_1L_2$, g) $L_2L_1$ and h) $L_2L_2$.

based on the evaluation system discussed in Section III. Figures 9(a) to 9(h) give a visual comparison of the generated disparity maps for multiwavelet subbands $L_1L_1$, $L_1L_2$, $L_2L_1$ and $L_2L_2$ of the 'Teddy' and 'Cones' stereo test images. The experimental results were generated using a number of multiwavelet types, i.e., balanced versus unbalanced, and symmetric-symmetric (SYM - SYM) versus symmetric - antisymmetric ( SYM - ASYM) multiwavelets (as listed in Table I). Table I shows the percentage of "bad pixels" at which the disparity error is larger than 1, for all regions (all). As it can be seen from the results presented in Table I, generally unbalanced multiwavelets give better results compared to the balanced multiwavelets. Furthermore, the symmetric-symmetric multiwavelets seem to produce slightly better results compared to symmetric-antisymmetric multiwavelets such as SA4. However, the symmetric - symmetric and symmetric-antisymmetric filter nature of multiwavelets doesn't seem to have a significant effect on the resulting disparity maps. The resulting disparity maps for balanced GHM and unbalanced BIGHM multiwavelets, applied to the 'Cones' and 'Teddy' test images are shown in Figures 10(a) and 10(b). From these figures, it is clear that the unbalanced multiwavelet based algorithm produces more accurate and smoother disparity maps compared to the balanced multiwavelet. This can be explained by the fact that the approximation subbands of the unbalanced multiwavelet carry different spectral content of the input images, which in turn enables the matching algorithm to generate more reliable matches.

TABLE I. EVALUATION RESULTS OF DIFFERENT MULTIWAVELETS IN STEREO CORRESPONDENCE MATCHING.

| **'TEDDY' (ALL)** | | | |
|---|---|---|---|
| ***Balanced Multiwavelets*** | | ***Unbalanced Multiwavelets*** | |
| CARDBAL2 | 9.78 | BIH32S | 8.82 |
| CARDBAL 3 | 9.54 | BIH52S (SYM-SYM) | 9.06 |
| BAT 01 | 9.98 | BIH34N | 8.82 |
| BAT02 | 9.69 | BIH54N (SYM-SYM) | 9.24 |
| GHM (SYM-SYM) | 10.35 | BIGHM | 8.91 |
| | | SA4 (SYM-ASYM) | 10.01 |
| **'CONES' (ALL)** | | | |
| ***Balanced Multiwavelets*** | | ***Unbalanced Multiwavelets*** | |
| CARDBAL2 | 9.82 | BIH32S | 9.65 |
| CARDBAL 3 | 9.40 | BIH52S (SYM-SYM) | 9.73 |
| BAT 01 | 10.23 | BIH34N | 9.65 |
| BAT02 | 9.77 | BIH54N (SYM-SYM) | 9.76 |
| GHM (SYM-SYM) | 10.59 | BIGHM | 9.45 |
| | | SA4 (SYM-ASYM) | 9.73 |

The performance of the proposed multiwavelet based GEEM technique has been evaluated against the 'Cones', 'Tsukuba', 'Teddy' and 'Venus' stereo test images. The performance of the proposed multiwavelet based GEEM algorithm is first benchmarked against similar GEEM algorithms operating in the spatial domain and respectively in the wavelet domain. A visual comparison of their performance is presented in Figure 11. The experimental results were generated using the GHM multiwavelet and the Antonini 9/7 scalar wavelet. The resulting disparity maps obtained using the proposed multiwavelet based algorithm, the wavelet based algorithm and respectively the GEEM technique applied to the original stereo views for the 'Teddy' and 'Cones' stereo pairs, are illustrated in Figures 11(a), 11(b) and 11(c) respectively. In these figures, areas with intensity zero represent occluded and unreliable disparities. As Figure 11 shows, the proposed multiwavelet based algorithm produces significantly more accurate and smoother disparity maps compared to both wavelet and spatial domain GEEM based algorithms. This can be explained by the multichannel structure of the multiwavelet transform, where the four resulting subbands carrying different spectral content of the input images, enable the global error energy minimization algorithm to generate more reliable matches. Operating on multiple channels with a narrower, more adaptive frequency spectrum split is certainly consistent with the structure of the human visual system itself, and from this point of view multiwavelets can be seen as a closer approximation of the human visual system than wavelets.

In order to give an objective quality comparison, the proposed algorithm is also evaluated against some well known techniques from the Middlebury database [22]. The results are presented in Table II. The chosen algorithms used for comparison are: AdaptingBP [23] (ranked second in the Middlebury database), DoubleBP [24] (ranked fourth in the Middlebury database), Graph Cut [25] and DP [26]. Table II shows the percentage of "bad pixels" at which the disparity error is bigger than 1. For each pair of images, the results in non-occluded regions (nonoc.), all regions (all) and depth discontinuity regions (disc.) are presented. From Table II, it

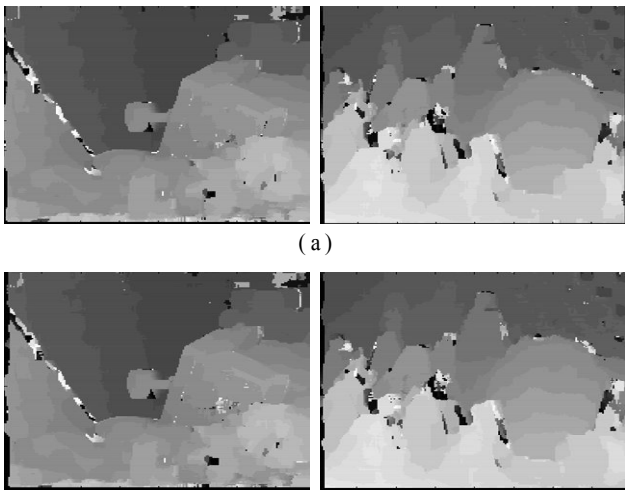

( a )

( b )

Figure 10. Disparity maps for 'Cones' and 'Teddy' stereo test image (a) unbalanced BIGHM and (b) balanced GHM multiwavelets.

can be seen that the multiwavelet based algorithm produces the second best results for 'Cones' and 'Teddy' stereo test images, while for 'Tsukuba' and 'Venus' it ranks third, and respectively third relative to the other four algorithms used for this comparison.

## VI. CONCLUSIONS

This paper presented an investigation into the application of different types and families of multiwavelets in the context of stereo correspondence matching. The paper introduced a new multiwavelet-based stereo matching technique which employs a global error energy minimization algorithm. For evaluation purposes, two correspondence matching algorithms were designed to deal with both balanced and unbalanced multiwavelets. In the case of balanced multiwavelets, due to the similar frequency content of the four multiwavelet approximation subbands, they were re-shuffled to generate one baseband and then normalized cross correlation was employed to generate a disparity map. In the case of unbalanced multiwavelets, normalized cross correlation was applied to the four resulting basebands leading to four disparity maps. These maps were then combined using a Fuzzy algorithm to form a single disparity map. The initial disparity map was then refined by hierarchically propagating it to the finer levels. The results generated using Middlebury stereo test images show that unbalanced multiwavelets work better than balanced ones for stereo correspondence matching, while the symmetric-symmetric and symmetric-antisymmetric nature of the multiwavelets doesn't have a significant effect in reducing erroneous matches.

This paper also introduced a hierarchical stereo matching technique based on multiwavelet transform and global error energy minimization algorithms. For one level of decomposition, a multiwavelet transform with multiplicity of 2, decomposes the input stereo images into 16 subbands. The resulting four approximation subbands of the two views were

TABLE II. EVALUATION RESULTS BASED ON THE ONLINE MIDDLEBURY STEREO BENCHMARK SYSTEM.

| ALGORITHM | 'TSUKUBA' | | |
|---|---|---|---|
| | NONOC. | ALL | DISC. |
| PROPOSED METHOD | 0.89 | 1.39 | 5.9 |
| ADAPTINGBP | 1.11 | 1.37 | 5.79 |
| DOUBLE BP | 0.88 | 1.29 | 4.76 |
| GRAPH CUT | 1.27 | 1.99 | 6.48 |
| DP | 4.12 | 5.04 | 12 |
| | 'VENUS' | | |
| PROPOSED METHOD | 2.59 | 2.61 | 2.02 |
| ADAPTINGBP | 0.1 | 0.21 | 1.44 |
| DOUBLE BP | 0.13 | 0.45 | 1.87 |
| GRAPH CUT | 2.79 | 3.13 | 3.6 |
| DP | 10.1 | 11 | 21 |
| | 'TEDDY' | | |
| PROPOSED METHOD | 6.45 | 7.12 | 9.31 |
| ADAPTINGBP | 4.22 | 7.06 | 11.8 |
| DOUBLE BP | 5.53 | 8.30 | 9.63 |
| GRAPH CUT | 12 | 17.6 | 22 |
| DP | 14 | 21.6 | 20.6 |
| | 'CONES' | | |
| PROPOSED METHOD | 7.25 | 8.09 | 10.66 |
| ADAPTINGBP | 2.48 | 7.92 | 7.37 |
| DOUBLE BP | 2.90 | 8.78 | 7.79 |
| GRAPH CUT | 4.89 | 11.8 | 12.1 |
| DP | 10.5 | 19.1 | 21.1 |

then used to generate a set of four disparity maps using a global error energy minimization algorithm. The resulting four disparity maps were then combined using a Fuzzy algorithm. The output of the Fuzzy combination algorithm constitutes the initial disparity map, which was then refined by hierarchically propagating it to the finer levels. Results show that the proposed technique produces a disparity map with significantly less mismatch errors compared to the same global error energy minimization algorithm applied to the original image data or to the wavelet transformed image data. The performance of the proposed multiwavelet based algorithm has been compared to other well-known techniques benchmarked and published in the Middlebury database. The results show that the proposed multiwavelet based algorithm fares well against many well established algorithms ranked at top positions in the Middlebury database. The multichannel nature of the multiwavelets and the different spectral content of the resulting subbands allow for greater correspondence matching flexibility than in the case of wavelets, and explain why the multiwavelet based technique performs better than when similar global error energy algorithms were applied in the wavelet and respectively the spatial domain.

## ACKNOWLEDGMENT

This work was supported by EPSRC under the EP/G029423/1 grant.

## REFERENCES

[1] P. Bagheri Zadeh and C. Serdean, "Stereo Correspondence Matching using Multi-Wavelets", 2010 Fifth International Conference on Digital Telecommunications (ICDT2010), Athens, Greece, pp. 153-157, June 2010.

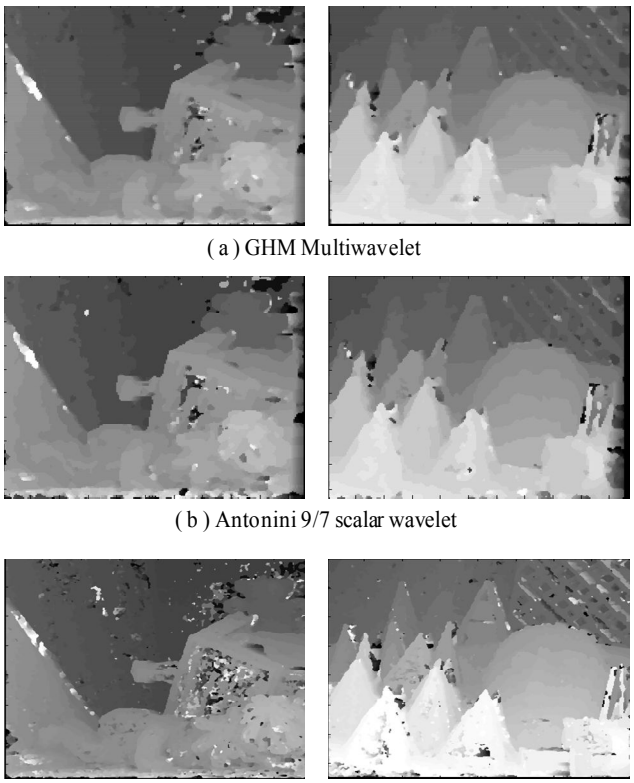

( a ) GHM Multiwavelet

( b ) Antonini 9/7 scalar wavelet

( c ) spatial domain

Figure 11. Disparity maps for 'Teddy' stereo test image (left) and 'Cones' stereo test image (right), using a) the proposed multiwavelet-based global energy minimization algorithm, b) the wavelet-based global energy minimization algorithm and c) global energy minimization algorithm in spatial domain.

[2] D. Scharstein and R. Szeliski, "A Taxonomy and Evaluation of Dense Two-Frame Stereo Correspondence Algorithms," International Journal of Computer Vision, vol. 47, pp. 7-42, April 2002.

[3] K. Muhlmann, D. Maier, R. Hesser, and R. Manner, "Calculating dense disparity maps from color stereo images, an efficient implementation," Proc. IEEE Workshop on Stereo and Multi-Baseline Vision (SMBV 2001), 2001, pp. 30-36 , doi: 10.1109/SMBV.2001.988760.

[4] L. Di Stefano, M. Marchionni, S. Mattoccia, and G. Neri, "A Fast Area-Based Stereo Matching Algorithm," Image and Vision Computing, vol. 22, pp. 983-1005, March 2004.

[5] S. Yoon, S. K. Park, S. Kang, and Y. Keun Kwak, "Fast correlation-based stereo matching with the reduction of systematic errors,"Pattern Recognition Letters, vol. 26 , pp. 2221-2231, October 2005.

[6] K.J. Yoon and I. S. Kweon, " Adaptive support-weight approach for correspondence search," IEEE Transactions on Pattern Analysis and Machine Intelligence, vol. 28, pp. 650-656, April 2006.

[7] H. Kim, S. Yang, and K. Sohn, " 3D reconstruction of stereo images for interaction between real and virtual worlds," Proc. IEEE International Conference on Mixed and Augmented Reality, October 2003.

[8] A.S. Ogale and Y. Aloimonos, "Robust Contrast Invariant Stereo Correspondence," Proc. IEEE International Conference on Robotics and Automation, ICRA 2005, pp. 819-824, April 2005.

[9] Q. Yang, L. Wang, R. Yang, S Wang, M. Liao, and D. Nister, "Real-time global stereo matching using hierarchical belief propagation", In Proceedings of the British Machine Vision Conference (BMVC), 2006.

[10] I. Choi and H. Jeong, "Fast Belief Propagation for Real-time Stereo Matching," International Conference on Advanced Communication Tech., ICACT 2009, pp. 1175-1179, Feburary 2009.

[11] S. Mallat, A Wavelet Tour of Signal Processing, Academic Press, 1999.

[12] V. Strela and A.T. Walden, "Signal and image denoising via wavelet thresholding: orthogonal and biorthogonal, scalar and multiple wavelet transforms," In. Nonlinear and Nonstationary Signal Processing, pp. 124-157, 1998.

[13] I. Sarkar and M. Bansal, "A wavelet-based multiresolution approch to solve the stereo correspondence problem using mutual information," IEEE Transaction on System, Man, and Cybernetics, vol. 37, pp. 1009-1014, August 2007.

[14] Q. Jiang, J. J. Lee, and M.H. Hayes, "A wavelet based stereo image coding algorithm," IEEE International Conference on Acoustics, Speech, and Signal Processing (ICASSP 99), vol.6, pp. 3157 - 3160, March 1999.

[15] G. Caspary and Y. Zeevi, "Wavelet-based multiresolution stereo vision," Proc. IEEE International Conference on Pattern Recognition (ICPR 2002), pp. 680- 683 , December 2002.

[16] A. Bhatti and S. Nahvandi, "Depth estimation using multi-wavelet analysis based stereo vision approach," International Journal of Wavelets, Multiresolution and Information Processing, vol. 6, pp. 481-497, 2008.

[17] V. Strela, "Multiwavelets: threory and applications," PhD thesis, MIT, 1996.

[18] J. Lian and C. K. Chui, "Balanced Multiwavelets With Short Filters," IEEE Signal Processing Letters, vol. 11, no. 2, pp. 75-78, Feb. 2004.

[19] L. Ghouti, A. Bouridane, M. K. Ibrahim, and S. Boussakta, "Digital Image Watermarking Using Balanced Multiwavelets," IEEE Trans. on Signal Pro. , Vol. 54, no. 4, pp. 1519-1536, 2006.

[20] B. B. Alagoz, "Obtaning depth maps from colour images by region based stereo matching algorithms," OncuBilim Algorithm and System Labs, vol. 08, Art.No:04, 2008.

[21] R.C. Gonzalez, R.E. Woods, and S.L. Eddins, Digital Image Processing second edition, Prentice Hall, pp. 75-142, 2002.

[22] http://vision.middlebury.edu/stereo/, last accessed June 2010.

[23] A. Klaus, M. Sormann, and K. Karner, "Segment-based stereo matching using belief propagation and a self-adapting dissimilarity measure," Proceedings of the 18th International Conference on Pattern Recognition (ICPR 2006), vol. 3, pp. 15-18, August 2006.

[24] Q. Yang, L. Wang, R. Yang, H. Stewenius, and D. Nister, "Stereo Matching with Color-Weighted Correlation, Hierarchical Belief Propagation, and Occlusion Handling," IEEE Transaction on Pattern Analysis and Machine Intelligence," Vol. 31, pp.1-13, March 2009.

[25] V. Kolmogorov and R. Zabih , "Multi-camera scene reconstruction via graph cuts," 7th European Conference on Computer Vision (ECCV 2002), pp. 8-40, May 2002.

[26] D. Scharstein and R. Szeliski, "A taxonomy and evaluation of dense two-frame stereo correspondence algorithms," International Journal of Computer Vision (IJCV 2002), Vol. 47, pp. 7-42 , April 2002.

[27] M.B. Martin, and A.E. Bell, "New image compression techniques multiwavelets and multiwavelet packets," IEEE Trans. Image Process. Vol. 10, no. 4, pp. 500–510, 2001.